Optical Guiding Properties of High-Brightness Parabolic Bow-Tie Laser Arrays

D. Masanotti and F. Causa, *Member, IEEE*

***Abstract*—This paper presents the characteristics of parabolic bow-tie laser arrays (PBTLAs) which are a novel category of laser diodes specially designed to achieve high power with high brightness at 980 nm. Output powers in excess of 2.8 W/facet have been measured from five-element PBTLAs with output beam less than twice the diffraction limit, achieving high brightness of 275 $\mathrm{MWcm^{-2}srad^{-1}}$ at 3 A (pulsed) injection current ($= 22$ times the threshold). Changes in the achievable brightness due to changes in the optical cavity geometry and in the lateral optical guiding strength are discussed in detail, using the coupled-mode theory to interpret the experimental results. At threshold all devices operate in the highest (double lobed) array mode. At higher currents the arrays of tapered lasers change to quasi-in-phase operation when the modal gain of the fundamental array mode dominates because of the combined effect of carrier hole burning and spatial filtering from the narrow stripe central section of the device. Similar trends have been observed under continuous-wave operation. The reduction of lateral optical guiding strength is deleterious for the operational characteristics of PBTLAs and linear bow-tie arrays, and it leads to filamentation in gain-guided devices even at low currents. Theoretical results presented in this paper show that scalability is in principle possible; however, changes in the lateral gain profile due to hole-burning can significantly increase the modal gain of higher order modes and, therefore, strongly influence the optical output profile.**

***Index Terms*—High-brightness laser arrays, high power, index- and gain-guiding, tapered geometry laser.**

I. Introduction

HIGH-POWER semiconductor optical sources that are characterized also by high brightness are now being used in a variety of applications including, for example, fiber amplifier and solid state laser optical pumping, free space communications, second harmonic generation, medicine, laser printing, lidar. To develop such semiconductor optical sources it is important to appropriately design both the material epitaxy and the device geometry. Tapered geometry devices seem to provide an effective design to combine the desirable operational characteristics of high power and narrow output beam with simple, low cost device fabrication. A useful classification of tapered devices can be made on the basis of the guiding properties of the structure, thus distinguishing between 1) diffraction-type devices, e.g., [1]–[4], where the beam freely diffracts in the homogeneous gain medium under the flared injection metal contact—the output beam from such devices is typically astigmatic and is focused using external optics to achieve diffraction-limited operation [1] and 2) index-guided devices [5]–[10], where an etched, tapered rib provides the explicit (weak) lateral waveguiding—the output beam quality in this case depends on the optical cavity geometry.

Of interest in this paper are devices of the latter category. Specifically it was found that index-guided parabolic bow-tie lasers (PBTLs) were well suited to achieve high brightness with moderately high-power output, [5], [7], [8]. However, to scale up the optical output power achieved with PBTLs it is not practical to simply increase the device dimensions to maintain the required adiabaticity. Therefore, parabolic bow-tie laser arrays (PBTLAs) were developed [9] to attain higher power and simultaneously higher brightness with a compact and low-cost device structure. Although arrays of semiconductor lasers are not a novelty, in the PBTL Arrays described in this paper the individual elements are coherently coupled with longitudinally nonuniform inter-element coupling. Further, as described in detail in Sections II–IV, the central spatial filtering section is of paramount importance to achieve in-phase locking to attain high power in a diffraction-limited output beam. In this context, the PBTLAs are different from other, more widely known, index-guided laser diode arrays including, for example, stripe laser arrays which tend to operate in the out-of-phase mode with the characteristic, unusable two-lobed beam pattern; or the arrays of linearly tapered lasers presented in [3], [4], [10], where the individual elements were intentionally uncoupled and high output power was achieved but in a nondiffraction limited output beam.

High-power continuous waves (CW) have been achieved at 980 nm with tapered lasers and amplifiers [1], [2] by using a system of lenses to focus the beam to nearly the diffraction-limit. On the other hand, with the PBTLAs described in this paper there is no need to use external lenses to collimate the beam since the index-guided cavity geometry has been designed to achieve diffraction-limited output. As a consequence the device size is compact and the device costs are reduced. In addition, a fundamental difference with respect to previously published arrays of tapered lasers is that the physical mechanism of operation of PBTLAs is based on coherent coupling which is weak along the length of the device, but strong at the facets to ensure stability of phase-locking. As discussed in this paper, scalability is in principle possible; however, changes in the lateral gain profile due to hole-burning can significantly increase the modal gain of higher order modes and, therefore, strongly influence the optical output profile.

The semiconductor material epitaxy and main device parameters are described in Section II. The design and the operational

Manuscript received November 16, 2004; revised January 27, 2005. This work was supported in part by the Engineering and Physical Sciences Research Council U.K.

The authors are with the Department of Electronic and Electrical Engineering, University of Bath, Bath BA2 7AY, U.K. (e-mail: D.Masanotti@bath.ac.uk; f.causa@bath.ac.uk).

Digital Object Identifier 10.1109/JQE.2005.848903

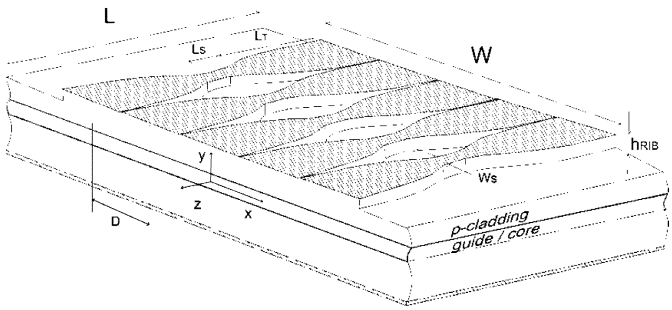

Fig. 1. Schematic of a five-element PBTLAs.

TABLE I
MATERIAL STRUCTURE

Layer	Composition	Thickness (μm)	Doping density (cm^{-3})	Dopant
Contact	GaAs	0.2	$3.0\ 10^{19}$	Zn
Cladding	$Al_{0.42}$	0.77	$8.0\ 10^{17}$	C
Guide	$Al_{0.20}$	0.24	undoped	--
QW	$In_{0.2}Ga_{0.8}As$	7nm	undoped	--
Barrier	GaAs	10nm	undoped	--
QW	$In_{0.2}Ga_{0.8}As$	7nm	undoped	--
Barrier	GaAs	10nm	undoped	--
QW	$In_{0.2}Ga_{0.8}As$	7nm	undoped	--
Guide	$Al_{0.20}$	0.24	undoped	--
Cladding	$Al_{0.42}$	1.77	$1.4\ 10^{18}$	Si
Buffer	GaAs	0.5	$1.4\ 10^{18}$	Si

characteristics of PBTLAs are discussed in Section III in the context of corresponding devices of different geometry to show that high-brightness operation can be achieved with a carefully designed optical cavity. Changes in the achievable brightness and filamentation characteristics due to changes in the lateral optical guiding strength are illustrated in Section IV, drawing the conclusions in Section V.

II. Device Structure and Main Characteristic Parameters

The schematic of a five-element PBTLA is given in Fig. 1 ($W = 100\ \mu$m, $D = 20\ \mu$m, $L = 1050\ \mu$m). The laser arrays were fabricated from a double heterostructure, large optical cavity (LOC), triple quantum well (TQW) semiconductor material specially designed for high-power operation at 980 nm, [7]. The epitaxial layer structure, Table I, was grown by low-pressure metal–organic vapor phase epitaxy on n-GaAs substrate. The main material and device parameters estimated from theory or experimental characterization are the following: (vertical) optical confinement factor in the TQW $\Gamma = 0.045$; equivalent spot size $S = (d/\Gamma) = 0.458\ \mu$m where d is the active region thickness; power density before COD $p_{\rm COD} = 11\ {\rm MWcm}^{-2}$; vertical beam divergence $\theta_y = 58^\circ$ which is in good agreement with that estimated theoretically for the given epitaxial structure [8].

The device geometry was optimized [8] to achieve high brightness also in the lateral (x) direction. The effective index method, was used to reduce the analysis to two dimensions (x, z) and, since the structure is weakly guiding, the scalar analysis was used to study the changes in lateral beam divergence, θ_x, with cavity geometry. Three different device geometries have been considered:

1) linear bow-tie laser (LBTL), for which $W(z) = W_S + ((W_o - W_S)/L_T)z$, where W_o is the facet width, Ws the width of the straight section and L_T the taper length, Fig. 1;
2) PBTL for which
$$W(z) = \sqrt{W_S^2 + \left(\left(W_o^2 - W_S^2\right)/L_T\right) z};$$
3) straight stripe laser (SL) for which $W(z) = W_o$.

All the devices of interest in this paper have the same width of the output facet $W_o = 20\ \mu$m and the same length $L = 1050\ \mu$m; for the tapered devices the straight section is characterized by $W_S = 3\ \mu$m and length $L_S = 50\ \mu$m.

The devices discussed in this paper present (tapered) ridges, Fig. 1, with the twofold purpose of reducing current spreading and producing an effective refractive index step necessary to provide weak (lateral) optical guiding. The strength of the lateral optical guiding depends on the material epitaxy and on the rib height $h_{\rm RIB}$. The LOC material used to fabricate the arrays has been specially designed to provide simultaneously high optical output power and sufficient lateral optical guiding with the appropriate rib height. In fact, the thickness of the guide layers is the critical parameter to be adjusted to satisfy the above two contradictory requirements [7]. In particular, devices characterized by a rib height $h_{\rm RIB} = 0.9\ \mu$m will be referred to in this paper as index-guided (IG) devices since the corresponding, estimated lateral effective index step $(\Delta n_{\rm eff} = 0.009)$ is sufficient to establish (weak) lateral optical waveguiding. This value of $h_{\rm RIB}$ was used to achieve diffraction limited operation from in-house fabricated PBTLs, as discussed in [7], [8]. By contrast, devices characterized by a shallower etched rib $(h_{\rm RIB} = 0.45\ \mu$m) will be referred to as gain-guided (GG) since the corresponding lateral effective refractive index step $(\Delta n \sim 0.0001)$ is negligible for lateral optical guiding. The shallow rib height of GG devices, however, is useful for reducing current spreading. The increased extent of current spreading compared to that occurring in IG devices, where the etched rib is deeper, is represented in Fig. 2. The theoretical current density and carrier density profiles for the individual IG- and corresponding GG-PBTLs are validated by experimental near field intensity profiles measured at low injection current $(I \ll I_{\rm th})$ with low-pass optical frequency filters to highlight the presence of the carriers at the device facet. The increased extent of current spreading in GG devices is reflected in the increased threshold current measured from such devices, as discussed in Section IV.

The tapered ridge waveguides were fabricated by ion beam etching with p-metal deposition by Ti–Au thermal evaporation in vacuum. The devices were cleaved and bonded p-side down on temperature stabilised $(T = 20\,^\circ{\rm C})$ copper mounts. Thermal management was not optimized and, therefore, the devices were tested predominantly using pulsed current with 0.1% duty cycle (200 Hz repetition rate, 5 μs pulse duration). However, preliminary results from CW measurements are also presented for completeness in Section III.

In Section III the operational characteristics measured from PBTLAs are compared with those measured from cor-

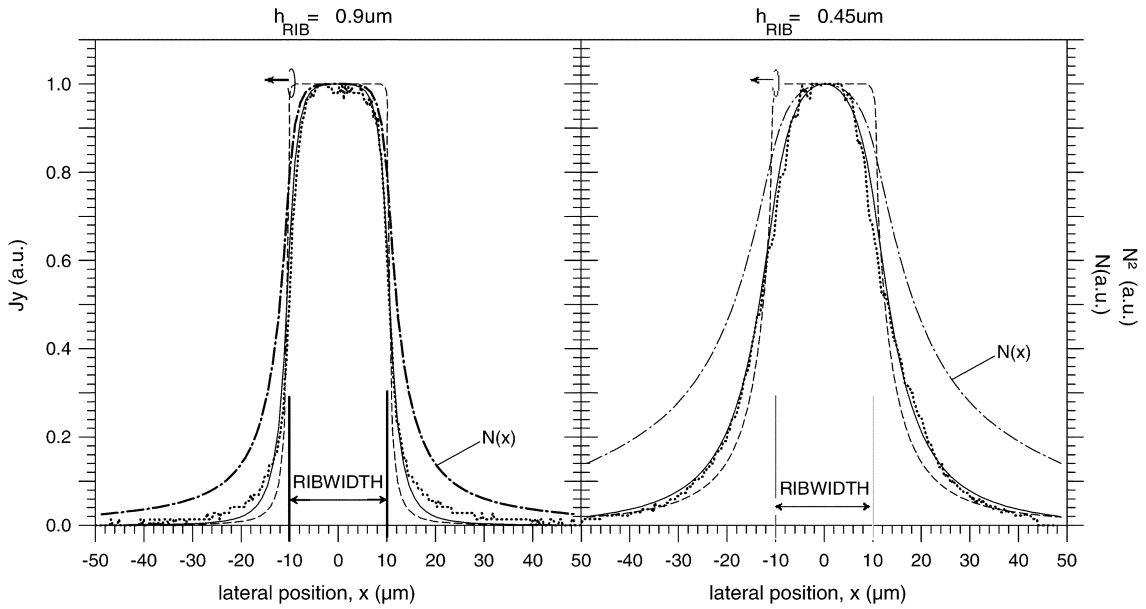

Fig. 2. Experimental near field intensity profiles (dotted line) measured at low injection current ($I \ll I_{\rm th}$) with low-pass optical frequency filters, and theoretically estimated current density (dashed line), carrier density (dash-dot line), and carrier density squared (solid line) profiles for IG and corresponding GG PBTLs.

responding arrays of five linearly tapered bow-tie lasers and SLs with same length and same output width, to show how the output beam quality is affected by the optical cavity geometry.

III. Index-Guided Arrays: Cavity Geometry Design to Achieve High Brightness

The results discussed in this section provide the justification for the use of a parabolic geometry optical cavity to achieve high brightness. The quality of the output beam is assessed by measuring not only the full-width at half-maximum (FWHM) of the far field intensity profile, but also the Strehl ratio (SR). The SR is defined as the fraction of power contained in a solid angle corresponding to the diffraction-limit angle for that particular device, and can be estimated experimentally by measuring the power through slits placed at the far field plane with aperture corresponding to the diffraction-limited divergence angle.

Representative optical and electrical (pulsed) characteristics measured from PBTLAs, linear bow-tie laser arrays (LBTLAs) and SLs are presented in Fig. 3. For all such devices the typical threshold current is $I_{\rm th} = 160$ mA, corresponding to threshold current density $J_{\rm th} = 0.2$ kAcm^{-2}; the slope efficiency is $\eta_{\rm slope} = 0.8$ WA^{-1}. Characteristic parameters including threshold current $(I_{\rm th})$, output power at $I = 22I_{\rm th}$, maximum (per pulse) wall-plug (W-P) efficiency, FWHM of the far field intensity profile, Strehl Ratio and corresponding estimated Brightness (B) measured from such devices at low $(I = 3I_{\rm th})$ and high $(I = 22I_{\rm th})$ currents are summarized for comparison in Table II.

Representative far field intensity profiles measured at different (pulsed) currents from the three categories of devices, without the use of external optics, are presented in Fig. 4. The angular resolution of the far field intensity measurements is $\sim 0.05^\circ$. It is interesting to note that at threshold all devices present a double-lobed pattern indicating out-of-phase mode operation. However, above threshold the quality of the output beam (and, therefore, the achievable brightness) changes significantly with the geometry of the optical cavity. Single-lobed

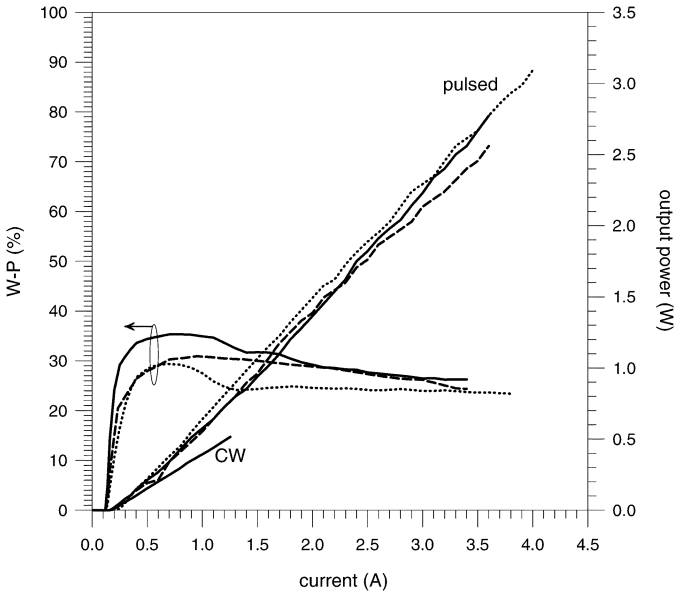

Fig. 3. Pulsed (5 μs, 200 Hz) L–I curves and W-P efficiency measured from in-house fabricated SLs (dotted line), LBTLAs (dashed line), and PBTLAs (solid line). The CW L–I curve from PBTLAs is also included for comparison. [Temperature: 20 °C. Neutral density filters used to take readings at high power levels].

TABLE II
Comparison of the Operational Characteristics Measured From In-House Fabricated SLs, LBTLAs, and PBTLAs Measured at $I = 3I_{\rm th}$ and at $I = 22I_{\rm th}$ Pulsed (5μs, 200 Hz)

	I_{th} (mA)	Max W-P (%)	Output Power (W/facet)		θ_{FWHM} (deg.)		B (MWcm^{-2}srad^{-1})		SR (%)	
			I=3I$_{th}$	I=22I$_{th}$	I=3I$_{th}$	I=22I$_{th}$	I=3I$_{th}$	I=22I$_{th}$	I=3I$_{th}$	I=22I$_{th}$
SL	220	29	0.17	3.1	9.1	13.8	5.0	25	0	0
LBTLA	160	31	0.23	2.6	2.0	3.1	8.4	92	30	20
PBTLA	160	35	0.32	2.8	0.8	1.08	42.4	275	65	40

output beams are obtained with arrays of tapered lasers, indicating that they operate quasi-in-phase (dominant fundamental array mode). By contrast, SLs are characterized by double-lobed far fields at all currents indicating that they are always locked out-of-phase. The change in mode operation at higher injection currents in tapered laser arrays is attributed to the effect of carriers on the refractive index and to gain hole-burning. Near the output facets, where the elements merge in a single contact, inter-element coupling is stronger. In those regions, above threshold, the refractive index on the longitudinal axis of the individual elements is larger, but the gain lower, than that of the surrounding off axis regions. This situation (higher modal gain for lower order array modes) is conducive to quasi-in-phase operation for arrays of a small number of elements [11]. The important, additional aspect to be considered for the arrays of coherently coupled bow-tie lasers discussed here is that the above effect is associated to the mode filtering effect of the central narrow stripe sections (Fig. 1) as demonstrated by the fact that in-phase locking is not observed in corresponding SLs.

The experimental measurements presented in this paper have been interpreted using results computed with theoretical models based on the coupled-mode theory (CMT) [12], [13]. Assuming that significant coupling between individual emitters occurs only at the device output facets, the array far field is calculated using as a starting point the optical field of an individual emitter calculated self-consistently [8], that is, including the effects of carrier diffusion and optical gain in the cavity. According to CMT an array of N weakly coupled identical elements is characterized by N array modes, also referred to as "supermodes" [12]. The far field of the array mode of order L, $F_L(\theta)$ [13] is given by

$$F_L(\theta) = |E(\theta)|^2 I_L(\theta) \tag{1}$$

where $E(\theta)$ is the far field amplitude of the individual emitter, $I_L(\theta)$ is the "grating function" which characterizes the effect of interelement-coupling on the array far field and $L = 1, 2, \ldots, N$ is the order of the array mode. The grating function is [13]

$$I_L(\theta) = \left\{ \frac{\sin\left(\frac{(N+1)u}{2} + \frac{L\pi}{2}\right)}{\left[\sin\left(\frac{u}{2}\right)\right]^2 - \left[\sin\left(\frac{L\pi}{2(N+1)}\right)\right]^2} \right\}^2 \tag{2}$$

where $u = k_0 D \sin(\theta)$, $k_0 = (2\pi/\lambda_0)$ is the free space propagation constant, and D is the (center-to-center) inter-element spacing (Fig. 1).

The array mode far field intensity profiles computed with the CMT model have been used to interpret the far fields measured from in-house fabricated arrays over a range of operating currents. As shown in Fig. 4, at threshold all experimental profiles are well represented by the highest order $(L = N)$ array mode which is generally referred to as the "out-of-phase" mode indicating that adjacent elements are operating out-of-phase [12], [13]. At higher currents the far fields of the arrays of tapered lasers become single-lobed, indicating quasi-in-phase mode operation, while those measured from SLs remain double-lobed. However, as is clear from the comparison between the fundamental array mode far field and the experimental profiles at high

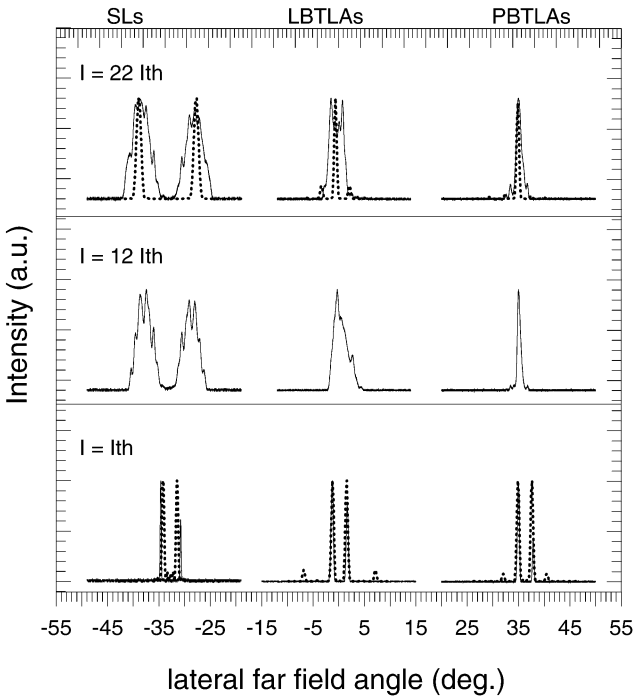

Fig. 4. Far-field intensity profiles measured (solid lines) without the use of external optics from index-guided SLs, LBTLAs, and PBTLAs at $I = I_{\rm th}$, $I = 12I_{\rm th}$ and $I = 22I_{\rm th}$ pulsed. The theoretical profiles calculated with CMT (dotted lines) are also included. [Angle resolution 0.05°].

currents (Fig. 4) although single-lobed, the far fields of both LBTLAs and PBTLAs are broader than expected revealing the contribution of higher order array modes, which explains the discrepancy between the measured far field FWHM (PBTLAs $\theta_{\rm FWHM} = 1.08°$; LBTLAs $\theta_{\rm FWHM} = 3.1°$) and the diffraction limit beam width $\theta_d = \arcsin(\lambda_o/W) = 0.56°$. In particular, although both arrays of tapered lasers, LBTLAs and PBTLAs, present essentially single-lobed far fields (i.e., quasi-in-phase mode operation) significantly higher brightness is achieved with PBTLAs $(B = 275\ \text{MWcm}^{-2}\text{srad}^{-1})$ compared to LBTLAs $(B = 95\ \text{MWcm}^{-2}\text{srad}^{-1})$, indicating that the parabolic geometry is more suited for high-brightness operation.

Theoretical results computed to analyze array mode discrimination in arrays as a function of the number of elements are presented in Fig. 5. As expected the modal gain of the fundamental $(L = 1)$ array mode is larger than that of the highest $(L = N)$ order mode when the gain in the region of higher refractive index is lower than that of the surrounding lower index region [Fig. 5(a) and (b)] [12]. This effect is noticeable experimentally in five-element PBTLAs above threshold. However, when hole-burning becomes significant and the gain of the central elements of the array is further reduced, the modal gain of the lowest and highest order modes decreases significantly with respect to that of other modes [Fig. 5(c)]. This effect is more noticeable for arrays of a large number of elements $(N > 8)$, whereas for arrays of a few elements (e.g., $N = 5$) the modal gain discrimination is less pronounced. Therefore, although scalability to a large number of elements is in principle possible, the changes in lateral gain profile due to hole-burning can be detrimental for the optical output profile. Preliminary measurements on PBTLAs with N up to 20 elements seem to

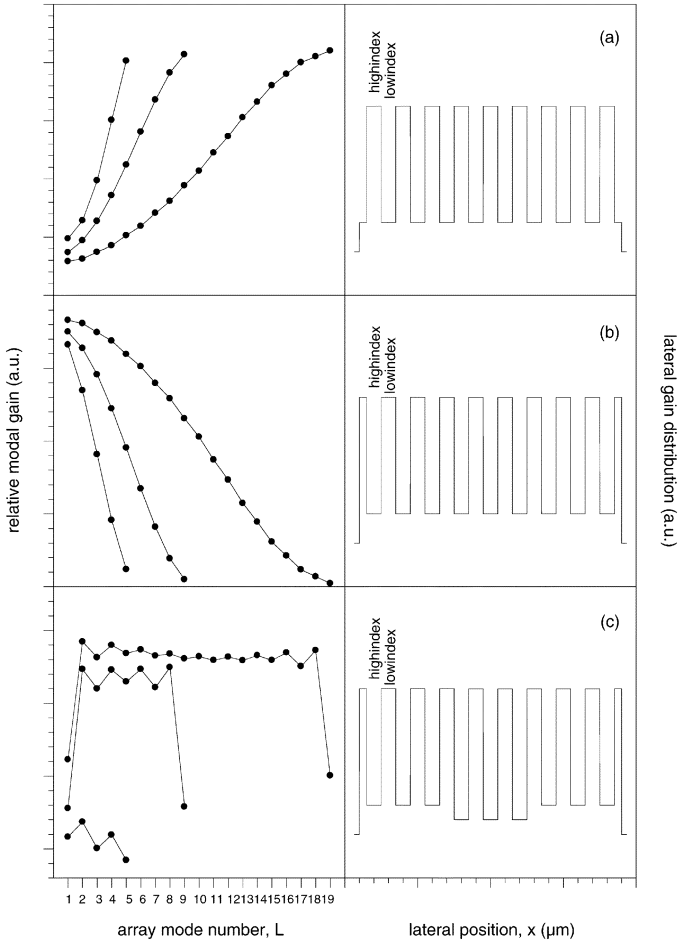

Fig. 5. Modal gain as a function of the mode number computed for arrays of five, nine, and 19 elements, for different gain profiles. (a) Highest gain in highest refractive index region. (b) Highest gain in lowest refractive index region. (c) Highest gain in lowest refractive index region in the presence of hole-burning at the center of the device. The lateral gain profiles are shown for array of $N = 9$ elements for clarity.

TABLE III
COMPARISON OF THE OPERATIONAL CHARACTERISTICS MEASURED FROM IN-HOUSE FABRICATED PBTLAS AT $I = 3I_{\rm th}$ AND $I = 7.5I_{\rm th}$ UNDER PULSED (5 μs, 200 HZ) AND CW OPERATION

	I_{th} (mA)	Max W-P (%)	Output Power (W/facet)		θ_{FWHM} (deg)		B (MWcm^{-2}srad^{-1})	
			$I = 3I_{th}$	$I = 7.5I_{th}$	$I = 3I_{th}$	$I = 7.5I_{th}$	$I = 3I_{th}$	$I = 7.5I_{th}$
pulsed	160	35	0.320	0.725	0.8	0.8	42.4	128
CW	160	20	0.190	0.515	3.2	3.0	5.4	12

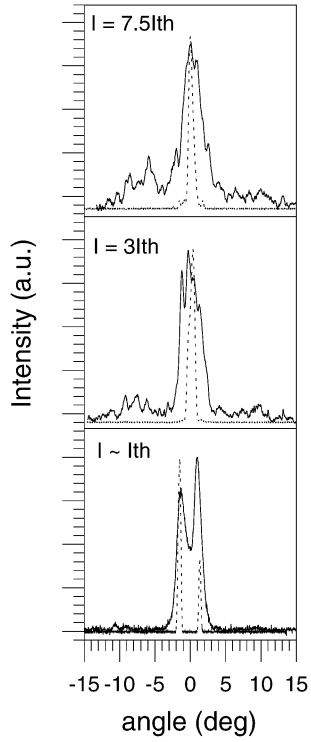

Fig. 6. Comparison of CW (solid line) and pulsed (dashed line) far-field intensity profiles measured from PBTLAs at different currents ($I \sim I_{\rm th}$, $I = 3I_{\rm th}$ and $I = 7.5I_{\rm th}$). Measurements taken without using external optics. [Angle resolution: 0.05°].

validate this statement since the measured far field is not diffraction-limited, but mainly single-lobed.

With the present experimental apparatus it is not possible to establish whether the devices are affected by beam steering because the accuracy of the scale of the far field measurement apparatus is 0.5°, which is of the same order of magnitude of reported values of beam steering [6], [14].

Preliminary results from CW measurements on PBTLAs confirm the trends observed under pulsed operation discussed above. Due to limitations in thermal management of the present experimental arrangement, the maximum CW driving current was restricted to $I = 1.2A = 7.5I_{\rm th}$. The main CW measurements results are summarized in Table III together with those obtained in pulsed conditions for PBTLAs. The threshold current is unchanged. However, the slope efficiency is reduced by approximately 25% and the W-P efficiency by 42%. This reduction in efficiency can be attributed to the present nonoptimal bonding and heat sink conditions. The T_0 parameter for the material of Table I used for laser fabrication has been extrapolated from CW L–I curves measured at temperatures between 15 °C and 60 °C and found to be $T_0 = 218$ °C, in agreement with expected values for semiconductor materials designed for emission in this wavelength range. As observed previously for the results taken in pulsed conditions, near threshold the far field presents two peaks, but becomes single-lobed above threshold (Fig. 6). However, the measured far field FWHM in CW ($\theta_{\rm FWHM} = 3°$) is broader than that obtained under pulsed conditions. As a consequence, the estimated brightness ($B = 12$ MWcm^{-2}srad^{-1}) is reduced by an order of magnitude with respect to that obtained under pulsed conditions, but it is still higher than that estimated for corresponding SLs ($B = 8.5$ MWcm^{-2}srad^{-1}) at the same CW injection current.

Compared to the more commonly used linear taper, the geometry of the parabolic taper is useful not only to achieve diffraction limited far field, but also to reduce optical feedback in the cavity at the narrow end of the tapered laser. The optical field profiles at the narrow end of an individual bow-tie laser computed for the linear and parabolic tapers [15], are compared in Fig. 7. From these results it is possible to conclude that cavity spoilers, e.g., [1], are not necessary in PBTLAs, but could be beneficial in LBTLAs.

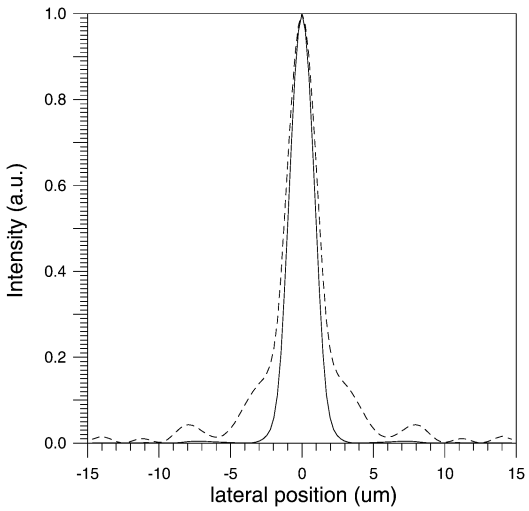

Fig. 7. Comparison of optical field intensity profile computed at the narrow end ($W = W_S$) of linear (dashed line) and parabolic (solid line) tapered lasers.

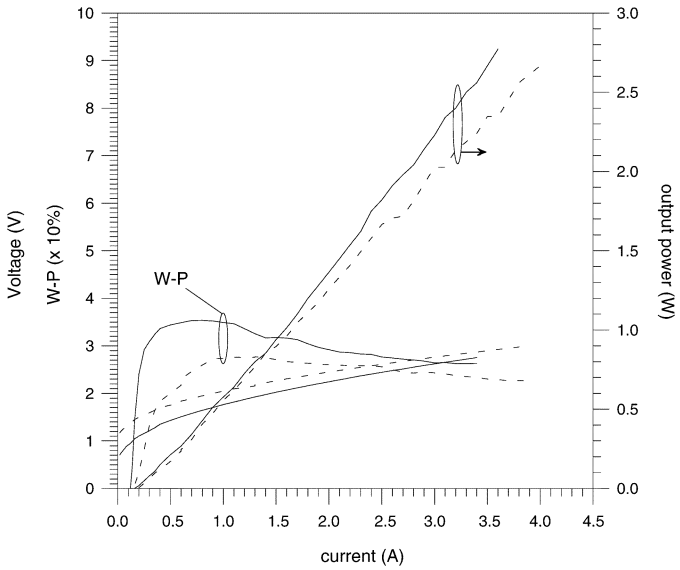

Fig. 8. L–I–V and W-P efficiency curves measured from IG- (solid line) and GG- (dotted line) PBTLAs. [5 μs pulse width, 200 Hz; Temperature: 20 °C. Intensity filters have been used to take readings at high power levels].

IV. Tapered Laser Arrays: Optical Guiding Strength

To analyze the effect of the lateral optical guiding strength on the device output power and brightness, GG devices with injection metal contact surface area identical to that of the IG devices discussed in Section III have been fabricated and characterized. Representative electrical and optical characteristics measured from IG- and GG-PBTLAs are compared in Fig. 8. As mentioned in Section II, because of the increased current spreading the threshold current of GG-PBTLAs, $(I_{\rm th})_{GG} = 200$ mA, is 25% higher than that measured for IG-PBTLAs, $(I_{\rm th})_{IG} = 160$ mA. The main operational characteristics measured from corresponding IG and GG PBTLAs are summarized in Table IV. From the opto-electrical point of view the distinction between IG- and GG-PBTLAs can be considered as marginal in terms of output optical power although GG devices are less efficient than corresponding IG arrays. The most important distinction

TABLE IV
Comparison of the Operational Characteristics Measured From In-House Fabricated IG- and GG- PBTLAs Measured at $I = 3I_{\rm th}$ and at $I = 22I_{\rm th}$ Pulsed (5 μs, 200 Hz). [R = Device Resistance]

	I_{th} (mA)	Max W-P (%)	η_{slope} (W/A)	R (Ω)	Output Power (W/facet)		θ_{FWHM} (deg.)		B (MWcm^{-2}srad^{-1})	
					I=3I$_{th}$	I=22I$_{th}$	I=3I$_{th}$	I=22I$_{th}$	I=3I$_{th}$	I=22I$_{th}$
IG	160	35	0.8	0.45	0.32	2.8	0.8	1.08	42.4	275
GG	200	29	0.7	0.33	0.24	3.0	filamentation		~0	~0

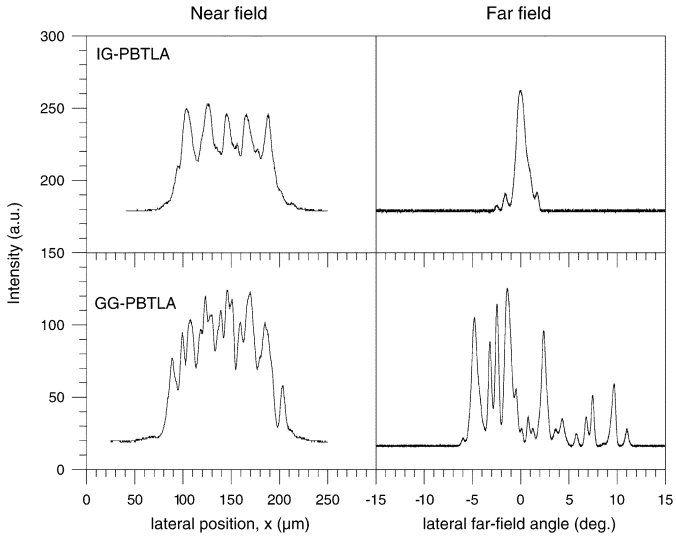

Fig. 9. Near- and far-field intensity profiles measured from IG- and GG-PBTLAs at $I = 22I_{\rm th}$ (pulsed).

between IG and GG devices in this context is that the light current characteristics of GG-PBTLAs present pronounced kinks which are associated with filamentation. In fact, filamentation is observed in both near- and far-field intensity profiles detected from GG devices. As a consequence, the output beam characteristics and, therefore, the achievable brightness from GG devices are dramatically different from those of IG devices.

Typical near field intensity profiles imaged at the facets of IG- and GG-PBTLAs above threshold $(I = 22I_{\rm th})$ are presented in the left-hand side of Fig. 9, where it is seen that the near field from GG devices presents visible irregularities. However, more significant information can be gathered from the corresponding far field intensity profiles, presented on the right-hand side of Fig. 9. Such far fields have been measured without the use of external optics, with an angular resolution of 0.05°. The output beam from GG-PBTLAs is multipeaked and shows evidence of filamentation at all currents above threshold.

To verify the presence of filamentation the following measurements have been taken on GG devices. The near field apparatus was used to detect the virtual beam waist (BW) by focusing the imaging lens inside the resonator to visualise the virtual beam origin. The resulting profiles from BW measurements are presented in Fig. 10. However, it is seen that although five BW spots (one per array element) are visible at injection currents up to about twice the threshold, the image becomes almost completely illegible at higher injection currents, as expected when filamentation occurs [16]. Further evidence of filamentation was provided by the comparison of near- and far-field intensity profiles from IG and GG PBTLAs and LBTLAs, with a view of

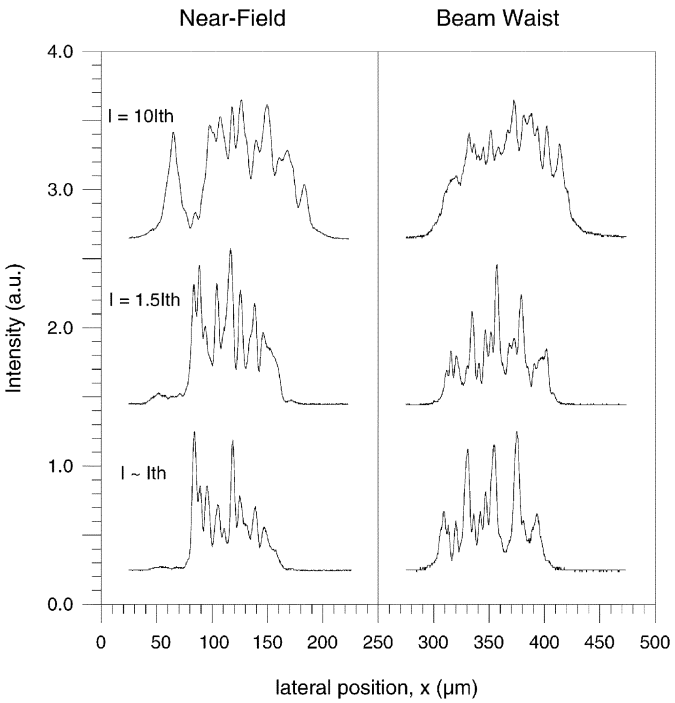

Fig. 10. Near field intensity profiles and corresponding BWs measured from GG-PBTLAs at different pulsed injection currents.

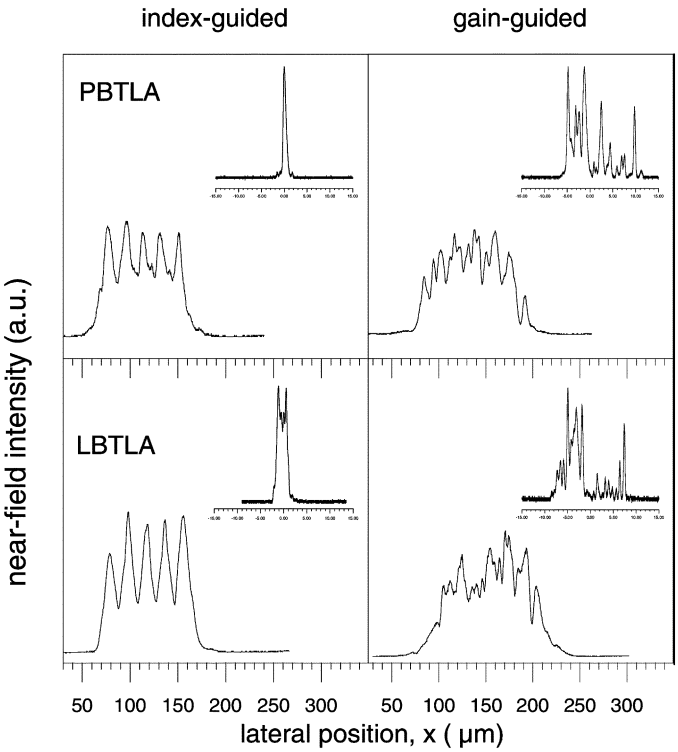

Fig. 11. Near field intensity profiles measured from IG- and GG- LBTLAs and PBTLAs at $I = 22I_{\rm th}$ (pulsed). Corresponding far field intensity profiles are presented in the insets.

detecting beam quality changes with changes in optical cavity geometry and index guiding strength. The results are presented in Fig. 11 where it is noted that the near- and far-field intensity profiles of GG devices of both geometries display similar characteristics, indicating (as expected) that the optical field is not affected by the taper geometry and that, therefore, above threshold the optical field freely propagating in the gain region is severely affected by filamentation. By contrast, as observed in Section III, the near- and far-field intensity profiles detected from the corresponding IG devices are significantly affected by the optical cavity design.

The longitudinal astigmatism for GG-devices has been estimated to be ~ 40 μm near threshold. However, at higher currents the astigmatism is not clearly quantifiable because, differently from properly designed GG-devices where the optical wave freely diffracts in the active medium, here the cavity does not permit free-diffraction of the optical beam and, therefore, filamentation becomes a dominant feature. Astigmatism was not observed in IG-devices.

V. Conclusions

The PBTLAs discussed in this paper are a novel category of high-power laser diodes with high brightness. The design and characterization of in-house designed and fabricated five-element arrays have been presented in detail to show that high-brightness operation can be achieved by careful optical cavity design. Changes in the achievable brightness due to changes in the optical cavity geometry and in the lateral optical guiding strength have been discussed. Theoretical results discussed in this paper show that scalability to a large number of elements is in principle possible; however, the changes in the lateral gain profile due to hole-burning can significantly increase the modal gain of higher order modes and, therefore, deteriorate the output beam profile.

Results computed with theoretical models based on the CMT have been used to interpret the experimental results. At threshold all experimental profiles are well represented by the highest order array mode; by contrast at higher currents, because of the effect of carriers on the refractive index and gain profiles and the mode filtering central section of the device, the far fields of the arrays of tapered lasers become single-lobed while those measured from SLs remain double-lobed. However, although single-lobed, the far fields of both LBTLAs and PBTLAs are broader than the desired diffraction-limit, revealing the contribution of higher order array modes. The estimated brightness from LBTLAs and PBTLAs is $B = 275\,\mathrm{MW}\cdot\mathrm{cm}^{-2}\mathrm{srad}^{-1}$ (output beam less than twice the diffraction limit), and $B = 95\,\mathrm{MW}\cdot\mathrm{cm}^{-2}\mathrm{srad}^{-1}$, respectively, indicating that the parabolic geometry is more suited for high-brightness operation. Preliminary results from CW measurements on PBTLAs confirm the trends observed from the pulsed measurements although lower efficiency and brightness are achieved in these conditions possibly due to the nonoptimal bonding and heat sinking conditions of the present devices. Finally, the loss of lateral optical guiding is deleterious for the operational characteristics of PBTLAs and LBTLAs. Filamentation was in fact observed in all gain-guided devices even at low currents.

Acknowledgment

The authors would like to thank Dr. J. S. Roberts (University of Sheffield, Sheffield, U.K.) for providing the required

semiconductor material, Mr. T. J. Ryan (Department Electronic and Electrical Engineering, University of Bath, Bath, U.K.) for device fabrication, Prof. J. N. Walpole for useful discussions, and the VI European Framework Programme LASER-LAB EUROPE (ref.: mbi000430) and the Max Born Institut fur Nichtlineare Optik und Kurzzeitspectroscopie for the use of their equipment to estimate T_0.

REFERENCES

[1] E. S. Kintzer, J. N. Walpole, S. R. Chinn, C. A. Wang, and L. J. Missaggia, "High power, strained-layer amplifiers and lasers with tapered gain regions," *IEEE Photon. Technol. Lett.*, vol. 5, no. 6, pp. 605–607, Jun. 1993.

[2] S. O'Brien, A. Shoenfelder, and R. J. Lang, "5-W CW diffraction-limited InGaAs broad area flared amplifier at 970 nm," *IEEE Photon. Technol. Lett.*, vol. 9, no. 9, pp. 1217–1219, Sep. 1997.

[3] M. Mikulla, A. Schmitt, M. Walther, R. Kiefer, W. Pletschen, J. Braunstein, and G. Weimann, "25-W CW high-brightness tapered semiconductor laser-array," *IEEE Photon. Technol. Lett.*, vol. 11, no. 4, pp. 412–414, Apr. 1999.

[4] J. S. Osinski, D. Mehuys, D. F. Welch, K. M. Dzurko, and R. J. Lang, "High-power, spectrally coherent arrays of monolithic flared amplifier-master oscillator power amplifiers (MFA-MOPAs)," *IEEE Photon. Technol. Lett.*, vol. 6, no. 10, pp. 1185–1187, Oct. 1994.

[5] N. S. Brooks, J. Sarma, and I. Middlemast, "A new design for tapered-geometry high-power semiconductor optical sources," in *Proc. Laser and Electro-Optics Society Annu. Meeting*, vol. 2, Nov. 1996, p. 207.

[6] M. Krakowski, S. C. Auzanneau, F. Berlie, M. Calligaro, Y. Robert, O. Parillaud, and M. Lecomte, "1 W high brightness index guided tapered laser at 980 nm using Al-free active region materials," *Electron. Lett.*, vol. 39, no. 15, pp. 1122–1122, 2003.

[7] D. Masanotti, F. Causa, and J. Sarma, "Design optimization of high power high brightness parabolic bow-lie laser diodes," *Proc. Inst. Elect. Eng. Circuits, Devices and Systems*, vol. 150, no. 6, pp. 537–561, 2003.

[8] ——, "High brightness, index-guided parabolic bow-tie laser diodes," *Proc. Inst. Elect. Eng. Optoelectronics*, vol. 151, no. 2, p. 123, 2004.

[9] F. Causa and D. Masanotti, "High brightness index-guided parabolic bow-tie laser arrays," *IEEE Photon. Technol. Lett.*, vol. 16, no. 9, pp. 2000–2002, Sep. 2004.

[10] F. J. Wilson, J. J. Lewandowski, B. K. Nayar, D. J. Robbins, P. J. Williams, N. Carr, and F. O. Robson, "9.5 W CW output power from high brightness 980 nm InGaAs/AlGaAs tapered laser arrays," *Electron. Lett.*, vol. 35, no. 1, pp. 43–44, 1999.

[11] H. Fujii, I. Suemune, and M. Yamanishi, "Analysis of transverse modes of phased-locked multistripe lasers," *Electron. Lett.*, vol. 21, no. 16, pp. 713–714, 1985.

[12] J. K. Butler, D. E. Ackley, and D. Botez, "Coupled-mode analysis of phase-locked injection laser arrays," *Appl. Phys. Lett.*, vol. 44, no. 3, pp. 293–295, Feb. 1984.

[13] D. Botez, "Array-mode far field patterns for phase-locked diode-laser arrays: Coupled-mode theory versus simple diffraction theory," *IEEE J. Quantum Electron.*, vol. QE-21, no. 11, pp. 1752–1755, Nov. 1985.

[14] W. D. Herzog, B. B. Goldberg, and M. S. Ünlü, "Beam steering in narrow-stripe high-power 980-nm laser diodes," *IEEE Photon. Technol. Lett.*, vol. 12, no. 12, pp. 1604–1606, Dec. 2000.

[15] F. Causa and J. Sarma, "A versatile method for analysing paraxial optical propagation in dielectric structures," *J. Lightw. Technol.*, vol. 18, no. 10, pp. 1445–1452, Oct. 2000.

[16] J. Guthre, G. L. Tan, M. Ohkubo, T. Fukushima, Y. Ikegami, T. Ijichi, M. Irikawa, R. S. Mand, and J. M. Xu, "Beam instability in 980 nm power lasers: Experiment and analysis," *IEEE Photon. Technol. Lett.*, vol. 6, no. 12, pp. 1409–1411, Dec. 1994.

D. Masanotti received the Laurea degree in electronic engineering from the University of Ancona, Ancona, Italy, in 1999. She is currently working toward the Ph.D. degree on the development of semiconductor lasers for high-power high-brightness operation at the Department of Electronic and Electrical Engineering, University of Bath, Bath, U.K.

In 1999, she joined the Department of Electronic and Electrical Engineering, University of Bath, as a Research Officer on a project for the development of Fabry–Pérot laser diodes for use in chaotic optical encryption experiments.

F. Causa (M'98) received the Laurea degree in physics from the University of Milan, Milan, Italy, in 1993 and the Ph.D. degree from the University of Bath, Bath, U.K., in 1998.

He joined the Department of Electronic and Electrical Engineering, University of Bath, as a Lecturer in 1999. Her research experience includes the modeling, design, and characterization of semiconductor optical devices. She has spent a period of secondment in industry sponsored by the Royal Academy of Engineering developing tapered geometry optical devices. In 2003, she visited the Tata Institute of Fundamental Research, Mumbai, India, as part of the British Council sponsored India–U.K. Young Scientist Networking Scheme. Her present research interests include the development of high-power lasers with high-brightness, high-power super-luminescent diodes, and modeling of nonlinear optical media.